

Concentration Effects in Polymer Solutions As Illuminated by Neutron Scattering

Robert Ullman*

Research Staff, Ford Motor Company, Dearborn, Michigan 48121

H. Benoit

Centre de Recherches sur les Macromolécules, 67083 Strasbourg Cedex, France

J. S. King

Department of Nuclear Engineering, University of Michigan, Ann Arbor, Michigan 48109.

Received May 10, 1985

ABSTRACT: Small-angle neutron scattering can be used to separate intramolecular and intermolecular contributions to scattering in polymer solutions. This has been carried through for the polystyrene-toluene system over a wide concentration range. The apparent homogeneity of the solution is a function of wave vector, and this is evident in this study. Also, the experiments are used to provide a critical evaluation of theoretical equations that have been proposed by Benoit and Benmouna and others.

Introduction

The scattering of radiation from a polymer solution arises from both intramolecular and intermolecular sources, which normally are inextricably mixed in an experiment. However, if some of the macromolecules are labeled such that their scattering cross sections are changed and their other physical and chemical properties are not, the intramolecular and intermolecular parts of the scattering function may be unscrambled. This is achieved by isotopic substitution in neutron scattering experiments. The replacement of hydrogen by deuterium on the polymer chain provides a practical procedure for achieving this goal.

Recently, we performed some small-angle neutron scattering studies on polystyrene in toluene from which radii of gyration and screening lengths were determined over a wide concentration range.¹ A great deal of additional information is contained in those scattering experiments, and it is our objective here to derive further insight from that investigation.

In 1948, Zimm² proposed an equation for light scattering from a polymer solution in which a "single-contact" approximation was used to obtain the primary influence of intermolecular interferences. The equation reads

$$I(\theta) = KcM[P(\theta) - 2A_2McP^2(\theta)] \quad (1)$$

$I(\theta)$ is the intensity of light scattered at an angle θ , K is a constant that includes a contrast factor and other constants, c is concentration in g/mL, M is molecular weight, $P(\theta)$ is a particle scattering factor, and A_2 is a second virial coefficient. This equation is correct, at best, to the order of c^2 and was based only on a limited class of polymer interactions.

If eq 1 is written in reciprocal form and higher powers of concentration are ignored, one obtains

$$Kc/I(\theta) = 1/MP(\theta) + 2A_2c \quad (2)$$

In an analysis based on a random-phase approximation, a result akin to eq 2 was obtained by Jannink and de Gennes.³ Their result differs from eq 2 in that it is designed for solutions of high concentration. In their result, A_2 of eq 2 is replaced by a covolume, which is a measure of the strength of the interaction between two monomer units on different molecules.

More recently, Benoit and Benmouna⁴ reanalyzed the problem. They arrived at eq 2 in two different ways: (a) by considering a large class of diagrams of molecular interactions, and (b) by invoking the Ornstein-Zernike

equation, which relates the direct and indirect correlation functions. As in the Jannink-de Gennes analysis, it is valid at high concentration, but it is also clear that it applies in the semidilute region as well. In ref 3 and 4 A_2 is replaced by an excluded volume quantity.

In our neutron scattering measurements of polystyrene in toluene, both $I(\theta)$ and $P(\theta)$ are measured. Consequently, it can be determined whether eq 2 is consistent with those results.

The range of correlated fluctuations in a polymer solution is determinable by a comparison of $I(\theta)$ and $P(\theta)$ as a function of both θ and concentration. There is no strict definition of fluctuation range that we apply, but since the total scattering intensity measures concentration fluctuations in a polymer solution, the relative magnitudes of $I(\theta)$ and $P(\theta)$ provide an estimate of local homogeneity of the solution on a molecular scale.

Equations of Neutron Scattering

In neutron scattering, the actual intensities measured are elastic and inelastic, incoherent and coherent. In ref 1, much effort was paid to the extraction of the coherent elastic scattering of the polymer from the total scattering. Here, only that coherent elastic scattering is discussed.

The theory of coherent scattering of neutrons from a polymer solution is identical with that of light scattering, but owing to the additional importance of fluctuations in isotopic composition, it is more convenient to adopt a slightly different language. We specify that the system contains a solvent plus protonated and deuterated polymer molecules. It is assumed that both protonated and deuterated molecules have the same degree of polymerization.

The intensity may be written as a function of \mathbf{q} , the wave vector, in two different useful ways. The magnitude of \mathbf{q} equals $(4\pi/\lambda) \sin(\theta)$, where λ is the wavelength of the neutrons and θ is the scattering angle. The intensity is^{5,6}

$$I(q) = \Phi[A_1S_s(q) + BS_T(q)] \quad (3a)$$

$$I(q) = \Phi[A_2S_s(q) + BS_p(q)] \quad (3b)$$

In these equations, Φ is a constant that takes both detector efficiency and instrumental geometry into consideration. $S_s(q)$ is a single-chain scattering function defined by

$$S_s(q) = 1/n^2 \sum_{ij} \langle \exp[i\mathbf{q} \cdot \mathbf{r}_{ij}] \rangle \quad (4a)$$

where \mathbf{r}_{ij} is the vector connecting monomer i with monomer j , n is the degree of polymerization, and the angular

Table I
 $S_s(q)$ and $S_T(q)/S_s(q)$ from Experiment B1^a as a Function of q (Å⁻¹) and c (g/mL)

| c | | q | | | | |
|------|-----------------|---------|---------|---------|---------|---------|
| | | 0.00758 | 0.01557 | 0.02379 | 0.03065 | 0.03996 |
| 0.04 | $S_s(q)$ | 0.790 | 0.448 | 0.231 | 0.139 | 0.0858 |
| 0.04 | $S_T(q)/S_s(q)$ | 0.160 | 0.234 | 0.399 | 0.585 | 0.792 |
| 0.06 | $S_s(q)$ | 0.837 | 0.464 | 0.248 | 0.144 | 0.0897 |
| 0.06 | $S_T(q)/S_s(q)$ | 0.103 | 0.160 | 0.270 | 0.388 | 0.510 |
| 0.08 | $S_s(q)$ | 0.837 | 0.471 | 0.255 | 0.164 | 0.101 |
| 0.08 | $S_T(q)/S_s(q)$ | 0.0759 | 0.114 | 0.189 | 0.279 | 0.388 |
| 0.12 | $S_s(q)$ | 0.824 | 0.493 | 0.276 | 0.173 | 0.103 |
| 0.12 | $S_T(q)/S_s(q)$ | 0.0416 | 0.0589 | 0.103 | 0.157 | 0.239 |
| 0.16 | $S_s(q)$ | 0.801 | 0.489 | 0.271 | 0.175 | 0.103 |
| 0.16 | $S_T(q)/S_s(q)$ | 0.0275 | 0.0476 | 0.0658 | 0.0951 | 0.158 |
| 0.22 | $S_s(q)$ | 0.793 | 0.496 | 0.285 | 0.179 | 0.104 |
| 0.22 | $S_T(q)/S_s(q)$ | 0.0195 | 0.0238 | 0.0401 | 0.0626 | 0.108 |

^a Calculated from measurements at $x = 0.5$ and $x = 0$.

Table II
 $S_s(q)$ and $S_T(q)/S_s(q)$ from Experiment B2^a as a Function of q (Å⁻¹) and c (g/mL)

| c | | q | | | | |
|------|-----------------|---------|---------|---------|---------|---------|
| | | 0.00700 | 0.01558 | 0.02319 | 0.03066 | 0.04040 |
| 0.02 | $S_s(q)$ | 0.855 | 0.403 | 0.212 | 0.128 | 0.0803 |
| 0.02 | $S_T(q)/S_s(q)$ | 0.307 | 0.499 | 0.697 | 0.778 | 0.860 |
| 0.03 | $S_s(q)$ | 0.814 | 0.403 | 0.220 | 0.122 | 0.0751 |
| 0.03 | $S_T(q)/S_s(q)$ | 0.207 | 0.352 | 0.501 | 0.726 | 0.830 |
| 0.04 | $S_s(q)$ | 0.813 | 0.418 | 0.223 | 0.133 | 0.0801 |
| 0.04 | $S_T(q)/S_s(q)$ | 0.149 | 0.249 | 0.388 | 0.553 | 0.681 |
| 0.06 | $S_s(q)$ | 0.805 | 0.420 | 0.229 | 0.134 | 0.0825 |
| 0.06 | $S_T(q)/S_s(q)$ | 0.0951 | 0.158 | 0.267 | 0.383 | 0.544 |
| 0.16 | $S_s(q)$ | 0.824 | 0.466 | 0.269 | 0.165 | 0.0900 |
| 0.16 | $S_T(q)/S_s(q)$ | 0.0307 | 0.0366 | 0.0580 | 0.101 | 0.176 |
| 0.22 | $S_s(q)$ | 0.814 | 0.481 | 0.273 | 0.167 | 0.0982 |
| 0.22 | $S_T(q)/S_s(q)$ | 0.0132 | 0.0192 | 0.0287 | 0.0464 | 0.0901 |

^a Calculated from measurements at $x = 0.5$ and $x = 0$.

brackets signify an average over all internal chain conformations. The pair scattering function is defined by

$$S_p(q) = (1/n^2N) \sum_{\substack{i,j \\ M \neq M'}} \langle \langle \exp[i\mathbf{q} \cdot \mathbf{r}_{ij}(M, M')] \rangle \rangle \quad (4b)$$

$\mathbf{r}_{ij}(M, M')$ is the vector that connects monomer i on molecule M with monomer j on molecule M' , there are N polymer molecules in the sample, and the double angular brackets represent an average over both the internal chain conformation and the intermolecular distribution. The total scattering function $S_T(q)$ is given by

$$S_T(q) = S_s(q) + S_p(q) \quad (4c)$$

which takes into account both intramolecular and intermolecular interactions. In the limit of low concentration $S_p(q)$ vanishes and $S_T(q) = S_s(q)$. The inclusion of the factor $1/N$ in the definition of $S_p(q)$ is designed so that $S_s(q)$, $S_p(q)$, and $S_T(q)$ are all of comparable magnitude.

The constants A_1 , A_2 , and B are

$$A_1 = (N_A c M / M_0^2) (a_H - a_D)^2 x (1 - x) \quad (5a)$$

$$A_2 = (N_A c M / M_0^2) [(a_D - a_s^*)^2 x + (a_H - a_s^*)^2 (1 - x)] \quad (5b)$$

$$B = (N_A c M / M_0^2) (a_p - a_s^*)^2 = A_2 - A_1 \quad (5c)$$

N_A is Avogadro's number, c is concentration in g/mL, M is the molecular weight of the polymer, and M_0 is the molecular weight of the monomer. The scattering lengths a_H and a_D are for the styrene and deuteriostyrene monomers, a_s^* is the scattering length of deuteriotoluene adjusted for the difference between the volume of a toluene molecule and the volume of a monomer unit in the polymer, and x is the mole fraction of polymer that is deuterated. a_p is the mean scattering length of the polymer,

defined by $a_p = a_D x + a_H (1 - x)$. At $x = 0$ or 1 , A_1 vanishes and the scattering is proportional to $S_T(q)$. Similarly, if the H/D ratio is chosen such that $a_p = a_s^*$, $B = 0$, and the scattering is proportional to the single-chain contribution, $S_s(q)$, only.

Experimental Materials and Procedures

The details are described in ref 1. The polymers were anionically prepared polystyrenes; the protonated sample had a weight-average molecular weight of 1.14×10^5 , the deuterated polymer, 1.11×10^5 . Both had M_w/M_n indices close to 1.05. The solvent in all cases was deuteriotoluene containing 99.6% + D. The scattering experiment was performed on the 30-m SANS spectrometer at Oak Ridge National Laboratory;^{7,8} the neutron wavelength was 4.75 Å. All measurements were corrected for incoherent scattering and instrumental variations.

Scattering experiments were carried out over a wide range of concentration between 0.02 g/mL and 100% polymer. The q range covered was from 0.007 to 0.07 Å⁻¹. $S_T(q)$ was determined from H-polymer in D-toluene; $S_s(q)$ was obtained from experiments with $x = 0.8$, where $a_p = a_s^*$, and by a linear combination of experiments at $x = 0.5$ and $x = 0$.

Qualitative Considerations

It is instructive to compare the relative magnitudes of $S_s(q)$ and $S_T(q)$. Recall that these functions are normalized such that $S_s(q)$ is the intramolecular fraction of $S_T(q)$. In Tables I and II, a list of values of $S_s(q)$ and $S_T(q)/S_s(q)$ at several values of q and over a wide concentration range is provided. It is important to bear in mind that $S_T(q)$ becomes small as the concentration increases, and, consequently, the relative errors in $S_T(q)$ become large. The data in Tables I and II include experiments at $x = 0.5$ and $x = 0$. The results at $x = 0.8$ are essentially the same.

Figure 1 contains plots of $S_T(q)/S_s(q)$ vs. concentration at several values of q . $S_T(q)/S_s(q)$ decreases rapidly with

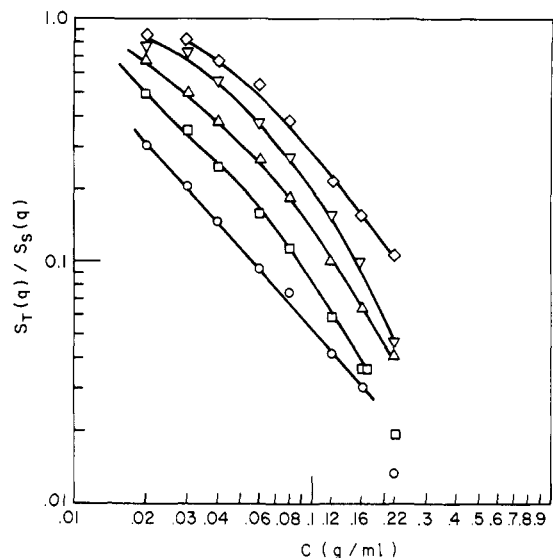


Figure 1. $S_T(q)/S_s(q)$ vs. c on a log-log scale for several values of q : (○) $q = 0.007$; (□) $q = 0.0156$; (Δ) $q = 0.0232$; (▽) $q = 0.0301$; (◇) $q = 0.0404$.

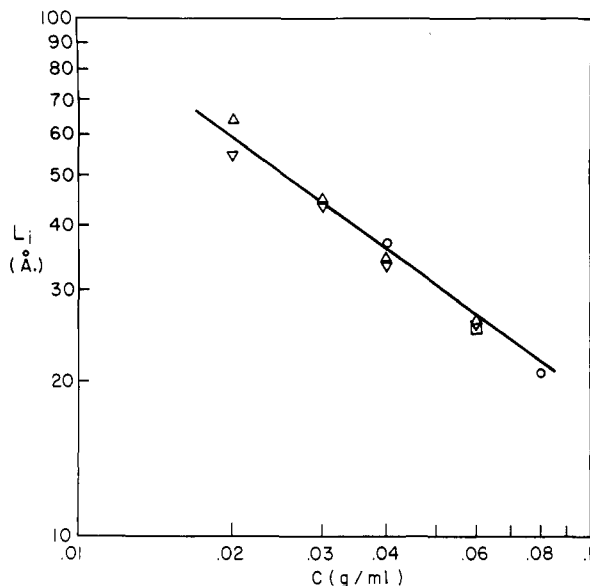


Figure 2. L_i vs. c on a log-log scale: (○) B1 experiment, $x = 0.5$; (□) B1 experiment, $x = 0.8$; (Δ) B2 experiment, $x = 0.5$; (▽) B2 experiment, $x = 0.8$.

concentration at constant q and increases with q at constant c . Since $S_T(q)/S_s(q) = 1 + S_p(q)/S_s(q)$, the relative intensities of intra- and intermolecular contributions can be seen at a glance from the plot. One can define for each concentration an interaction length that is the value of q^{-1} at which the magnitudes of the total scattering ($S_T(q)$) and intermolecular contributions to the scattering ($S_p(q)$) are equal. That interaction length, L_i , is plotted vs. c in Figure 2 on a log-log plot. A best line through the points is given by $L_i = 3.44c^{-0.73 \pm 0.03}$. L_i is defined in terms of the relative magnitude of intra- and intermolecular terms in the scattering function and does not depend on any presumed radial distribution of segments. It is roughly comparable in magnitude to the screening length, which for these solutions (see ref 1) satisfies the equation $\xi = 2.89c^{-0.70}$.

Analysis according to the Benoit-Benmouna Equations

Equation 13a of ref 4 may be written in the notation of this paper as

$$S_T(q) = S_s(q)/(1 + (N_A Mc/M_0^2)\nu S_s(q)) \quad (6a)$$

Table III
Slopes and Intercepts from Plots of $(S_T(q))^{-1}$ vs. $(S_s(q))^{-1}$

| c , g/mL | x | slope | error in slope | intercept | error in intercept |
|---|-----|-------|----------------|--------------------|--------------------|
| B1 Experiments: $0.011 \leq q \leq 0.050$ | | | | | |
| 0.04 | 0.5 | 0.56 | 0.014 | 8.20 | 0.14 |
| 0.04 | 0.8 | 0.65 | 0.014 | 7.91 | 0.13 |
| 0.06 | 0.5 | 0.79 | 0.015 | 12.14 ^a | 0.13 |
| 0.06 | 0.8 | 0.82 | 0.014 | 12.12 ^a | 0.13 |
| 0.08 | 0.5 | 0.74 | 0.017 | 17.66 ^a | 0.14 |
| 0.12 | 0.5 | 0.88 | 0.038 | 32.32 ^a | 0.31 |
| 0.12 | 0.8 | 0.90 | 0.037 | 32.19 ^a | 0.30 |
| 0.16 | 0.5 | 0.79 | 0.094 | 53.73 ^a | 0.77 |
| 0.16 | 0.8 | 0.82 | 0.096 | 53.63 ^a | 0.77 |
| 0.22 | 0.5 | 1.32 | 0.190 | 81.36 | 1.48 |
| 0.22 | 0.8 | 1.38 | 0.196 | 81.25 | 1.48 |
| B2 Experiments: $0.011 \leq q \leq 0.047$ | | | | | |
| 0.02 | 0.5 | 0.92 | 0.020 | 2.72 | 0.19 |
| 0.02 | 0.8 | 1.17 | 0.037 | 2.05 | 0.29 |
| 0.03 | 0.5 | 0.80 | 0.015 | 5.23 ^a | 0.15 |
| 0.03 | 0.8 | 0.83 | 0.017 | 5.05 ^a | 0.17 |
| 0.04 | 0.5 | 0.88 | 0.010 | 7.41 ^a | 0.09 |
| 0.04 | 0.8 | 0.98 | 0.019 | 7.16 ^a | 0.17 |
| 0.06 | 0.5 | 0.76 | 0.015 | 13.17 ^a | 0.14 |
| 0.06 | 0.8 | 0.83 | 0.019 | 12.95 ^a | 0.17 |
| 0.16 | 0.5 | 0.92 | 0.11 | 56.3 ^a | 0.92 |
| 0.16 | 0.8 | 0.92 | 0.11 | 56.4 ^a | 0.91 |
| 0.22 | 0.5 | 1.37 | 0.41 | 105 | 3.14 |
| 0.22 | 0.8 | 1.41 | 0.41 | 104 | 3.07 |

^a Points used for calculating the "best" line in Figure 9.

The quantity ν is an excluded volume interaction parameter that vanishes in the Θ state and is positive in a good solvent. In reciprocal form, eq 6a becomes

$$(S_T(q))^{-1} = (S_s(q))^{-1} + (N_A Mc/M_0^2)\nu \quad (6b)$$

The form of eq 6b is identical with that of eq 2. However, it is developed for use over a wide range of concentrations and not only at low concentration, to which eq 2 was restricted, according to Zimm's derivation.

One method of verification of the validity of eq 6a and 6b is to plot $(S_T(q))^{-1}$ vs. $(S_s(q))^{-1}$. We have done this for many samples, and the slopes and intercepts are set down in Table III. Included in the table are estimates of the errors in the slopes and intercepts based on the distribution of the points about the best line.

The largest errors, both random and systematic, are in $(S_T(q))^{-1}$, especially at the higher concentrations and also at higher q . The reliability of the results can be estimated by comparing numerical values of the slopes of the B1 and B2 experiments at the same concentration. The experiments carried out at $c = 0.04$ g/mL in the B1 series appear to be exceptional. This can be traced to slightly high values of $S_T(q)$ in the B1 experiment, the origin of which is unclear. In Figures 3–5, sample graphs of $(S_T(q))^{-1}$ vs. $(S_s(q))^{-1}$ are presented. While experiments were also performed at $c = 0.35$ and 0.50 g/mL, the fluctuations in $S_T(q)$ were too great for the results to be useful.

The validity of eq 6b can also be tested by plotting $\nu(q)$ (defined as $(S_T(q))^{-1} - (S_s(q))^{-1} / (N_A Mc/M_0^2)$) vs. q . If eq 6b were correct, the graph would be a line parallel to the abscissa. Figures 6–8 present typical examples. A deviation from the predicted result is clearly evident in Figure 6, though agreement between experiment and theory is satisfactory in Figures 7 and 8. A useful way to look at the data is to calculate an average value of ν (eq 6b), which is designated by $\bar{\nu}$, to measure the change in ν between the lower and upper values of q from the best lines shown in the graphs and to calculate the relative change in ν over the region of q used for the calculation. This relative change $(\nu(q_2) - \nu(q_1))/\bar{\nu}$, $(\Delta\nu/\bar{\nu})$ together with $\bar{\nu}$ is pres-

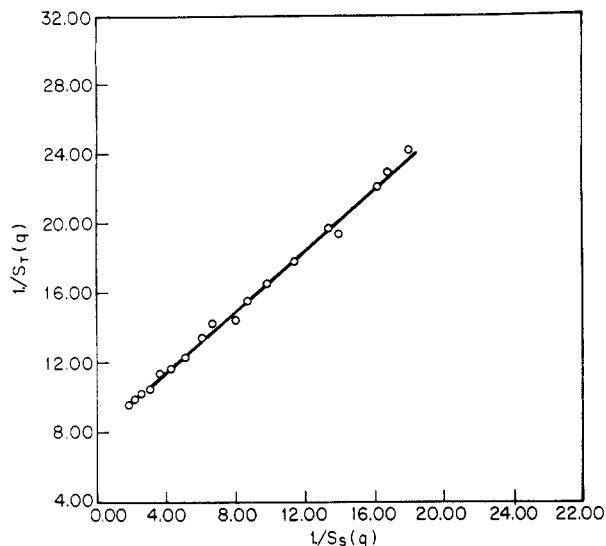


Figure 3. $(S_T(q))^{-1}$ vs. $(S_s(q))^{-1}$: B2 experiment; $c = 0.04$ g/mL; $x = 0.5$.

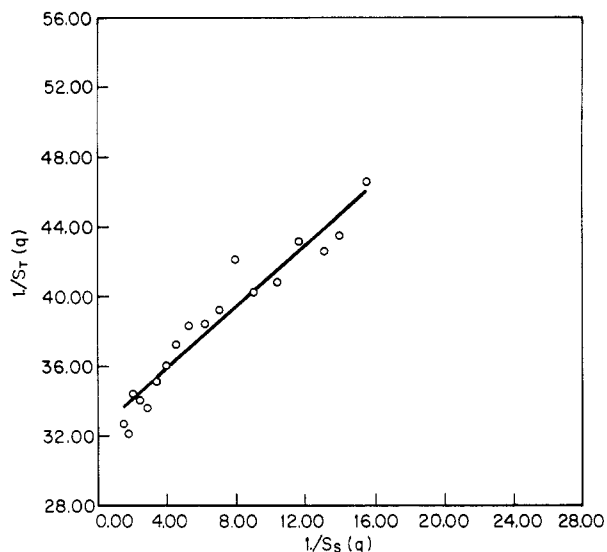


Figure 4. $(S_T(q))^{-1}$ vs. $(S_s(q))^{-1}$: B1 experiment; $c = 0.12$ g/mL; $x = 0.5$.

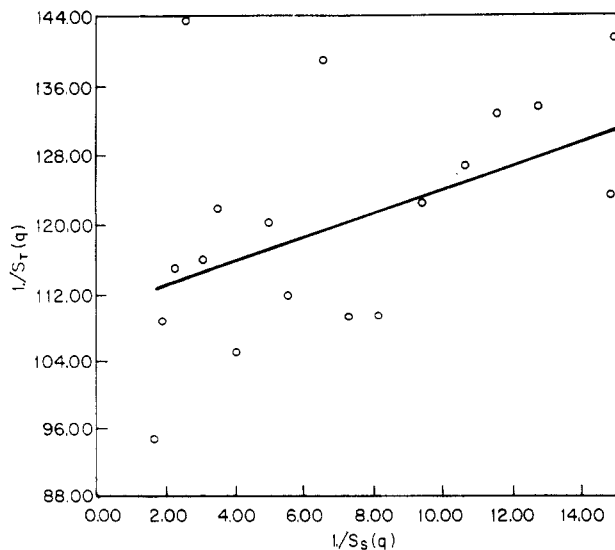


Figure 5. $(S_T(q))^{-1}$ vs. $(S_s(q))^{-1}$: B2 experiment; $c = 0.22$ g/mL; $x = 0.5$.

ented in Table IV for both the B1 and B2 series of experiments.

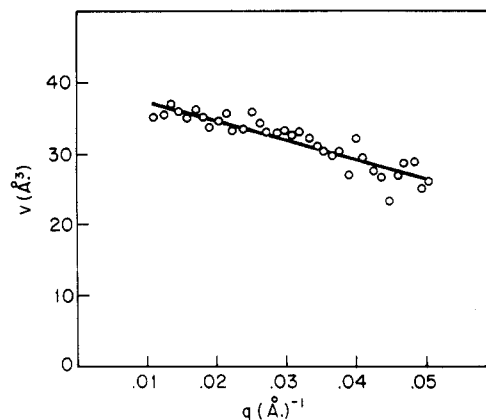


Figure 6. v ($\text{\AA}^3/\text{monomer}$) vs. q : B1 experiment; $c = 0.06$ g/mL; $x = 0.5$.

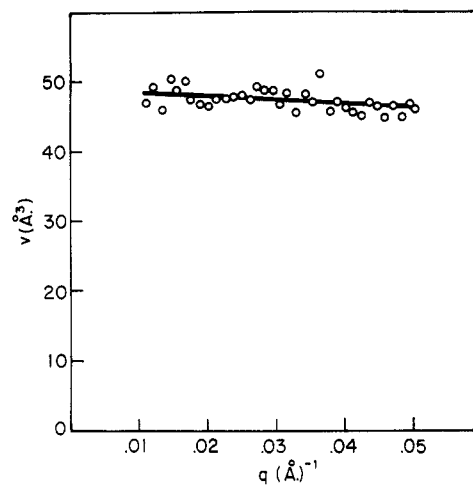


Figure 7. v ($\text{\AA}^3/\text{monomer}$) vs. q : B1 experiment; $c = 0.12$ g/mL; $x = 0.5$.

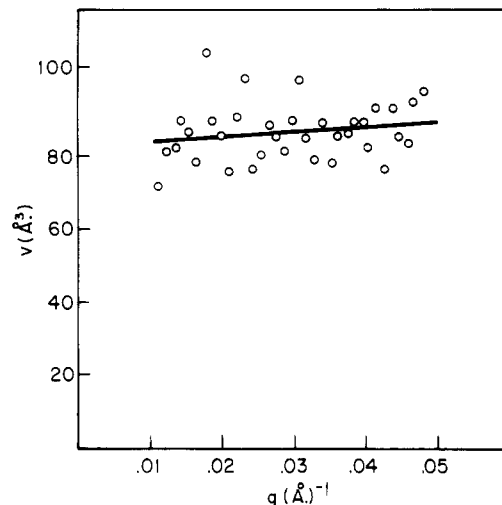


Figure 8. v ($\text{\AA}^3/\text{monomer}$) vs. q : B2 experiment; $c = 0.16$ g/mL; $x = 0.5$.

Discussion

In this investigation, the scattering from the solution has been separated into single-chain and pair contributions. In Tables I and II, it is shown that, while the single-chain scattering changes only modestly with concentration, reflecting small changes in molecular size, the total scattering decreases rapidly. It follows that the pair scattering is negative and approaches the single-chain term in magnitude as concentration increases. The intermingling of polymer chains washes out concentration fluctuations,

Table IV
Excluded Volume Parameter \bar{v} and Its Apparent Variation with Concentration^a

| c , g/mL | x | series B1 | | series B2 | |
|------------|-----|-------------------|--------------------|-------------------|--------------------|
| | | \bar{v} | $\Delta v/\bar{v}$ | \bar{v} | $\Delta v/\bar{v}$ |
| 0.02 | 0.5 | | | 20.9 | -0.63 |
| 0.02 | 0.8 | | | 33.0 | 0.71 |
| 0.03 | 0.5 | | | 23.8 ^b | -0.99 |
| 0.03 | 0.8 | | | 24.7 ^b | -0.76 |
| 0.04 | 0.5 | 24.5 | -1.70 | 33.2 ^b | -0.29 |
| 0.04 | 0.8 | 28.0 | -1.08 | 35.7 ^b | -0.04 |
| 0.06 | 0.5 | 37.2 ^b | -0.33 | 38.3 ^b | -0.33 |
| 0.06 | 0.8 | 38.1 ^b | -0.26 | 39.7 ^b | -0.20 |
| 0.08 | 0.5 | 42.0 ^b | -0.24 | | |
| 0.12 | 0.5 | 55.6 ^b | -0.049 | | |
| 0.12 | 0.8 | 55.5 ^b | -0.044 | | |
| 0.16 | 0.5 | 70.5 ^b | -0.040 | 70.2 ^b | -0.012 |
| 0.16 | 0.8 | 69.0 ^b | -0.035 | 70.3 ^b | -0.011 |
| 0.22 | 0.5 | 79.4 | -0.067 | 97.1 | 0.051 |
| 0.22 | 0.8 | 79.6 | -0.073 | 97.2 | 0.052 |

^aFor series B1 $q_1 = 0.01105$ and $q_2 = 0.05047$. For series B2 $q_1 = 0.01135$ and $q_2 = 0.04789$. The data analysis is based upon measurements over a range of wave vector beginning at q_1 and ending at q_2 . ^bPoints used for calculating the "best" line in Figure 10.

causing the system to be nearly homogeneous on the scale of q^{-1} at higher concentrations. This is also evident in the increase of $S_T(q)/S_s(q)$ with q at constant concentration. Stated in another way, when viewed on a small scale (smaller q^{-1} , larger q), the concentration fluctuations become visible. The data in Tables I and II and Figure 1 assign numbers to its magnitude. The interaction length L_i provides a parametric measure of the effect.

The osmotic pressure of a solution can be written in a virial expansion

$$\Pi = (RT/M)c + A_2c^2 + A_3c^3 + \dots \quad (7a)$$

The virial expansion does not converge at high concentration, and in semidilute solution, according to des Cloizeaux⁹

$$\Pi \sim c^{(3\nu/(3\nu-1))} \quad (7b)$$

where ν is the exponent in the relation between molecular dimensions and molecular weight $R_g \sim M^\nu$, R_g being a radius of gyration. A classical result of scattering theory states that $S_T(0)$ is proportional to $(\partial\Pi/\partial c)^{-1}$,^{10,11} which, together with eq 7a, yields

$$(S_T(0))^{-1} = (X_s(0))^{-1} + 2(A_2M/RT)c + 3(A_3M/RT)c^2 + \dots \quad (8a)$$

des Cloizeaux's law (eq 7b) applies strictly in the limit of high molecular weight where the first term on the right of eq 7a is vanishingly small. This is not correct for the polymer used in these experiments, particularly at low concentration. $S_s(0)$ is unity by definition; $(S_T(0))^{-1}$, at each concentration, is listed as the intercept in Table III. In view of eq 8a, a modified form of des Cloizeaux's law for a polymer of finite molecular weight takes the form

$$(S_T(0))^{-1} = 1 + Kc^{1/(3\nu-1)} \quad (8b)$$

K is a constant of proportionality. By comparing eq 6b in the limit $q = 0$ with eq 8b, one arrives at

$$\nu(0) \sim c^{(2-3\nu)/(3\nu-1)} \quad (9)$$

The classical excluded volume theory¹² predicts that $\nu = 0.6$, and a renormalization calculation¹³ arrives at $\nu = 0.588$. Einaga et al.¹⁴ performed intrinsic viscosity experiments on polystyrene solutions in cyclohexane and benzene. Analysis of those results led to a value of $\nu = 0.57$ (see ref 1) for polystyrene of molecular weight 10^5 . Using these

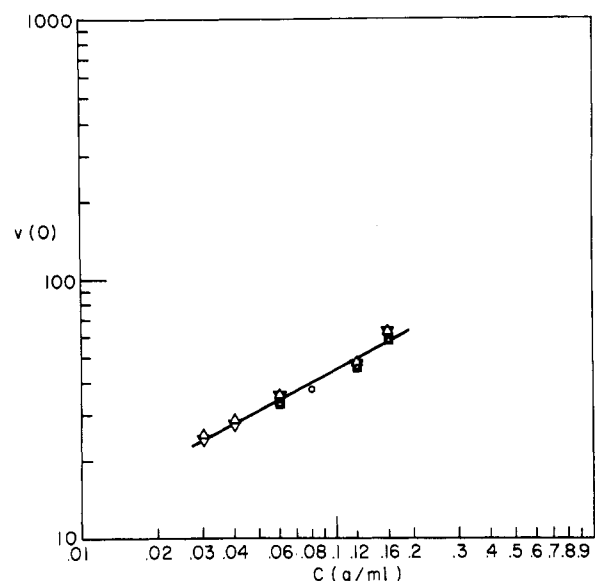


Figure 9. $\nu(0)$ vs. c : (O) B1 experiment, $x = 0.5$; (□) B1 experiment, $x = 0.8$; (Δ) B2 experiment, $x = 0.5$; (▽) B2 experiment, $x = 0.8$.

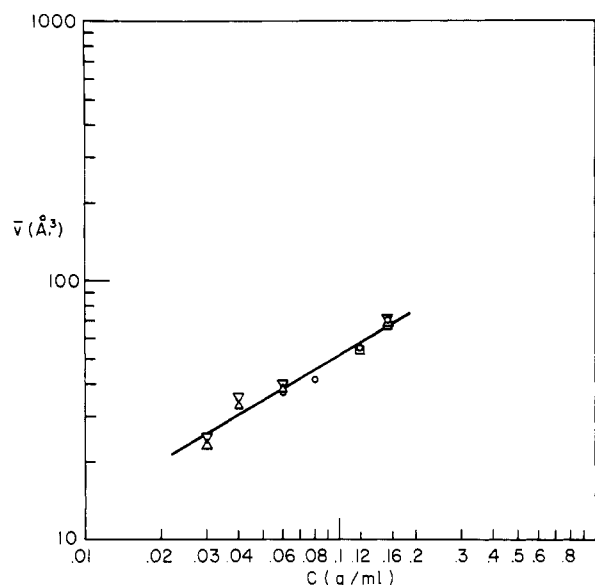


Figure 10. \bar{v} vs. c : (O) B1 experiment, $x = 0.5$; (□) B1 experiment, $x = 0.8$; (Δ) B2 experiment, $x = 0.5$; (▽) B2 experiment, $x = 0.8$.

three results in eq 9 yields $\nu(0) \sim c^{0.25}$, $c^{0.31}$, and $c^{0.41}$, respectively. The experimental determination, obtained from a fit to a log-log plot in Figure 9, yields $\nu(0) = 152c^{0.53 \pm 0.03}$, roughly consistent with the value of ν extracted from the experiments in ref 14.

The quantity \bar{v} , presented as a function of concentration in Table IV, is similar to, but not identical with, $\nu(0)$. It obeys a similar power law: $\bar{v} \sim c^{0.58 \pm 0.03}$. The results are exhibited in Figure 10.

Equations 6a and 6b, which relate $S_T(q)$ to $S_s(q)$, were derived for solutions in which molecular overlap is substantial.^{3,4} The criterion on substantial overlap is not met by the more dilute solutions studied here, and some of the difference between experiment and theory may be due to questionable applicability of the theory over the entire range. Of course, there are, in addition, experimental errors, which are large at both the high- and low-concentration limits. Some idea of the magnitude of these errors can be obtained by observation of Figures 3–8 and from the estimated statistical errors of the slopes and intercepts in Table III. Systematic experimental errors undoubtedly

exist and are difficult to identify, but to our knowledge these are not large enough to account for differences between theory and experiment.

It is expected that mean field estimates of molecular interaction are inexact, and we regard the approximate concord between experiment and theory as quite satisfactory. It is not surprising that the parameter ν depends slightly on q , even though a strict application of the theory demands that it be independent of q . The results in the tables and figures provide a first estimate of the validity of this theoretical model.

Summary and Conclusions

1. Small-angle neutron scattering studies of polystyrene and its deuterated homologue in deuteriotoluene have been analyzed so that intermolecular and intramolecular contributions are clearly separated. The experiments were performed over a wide concentration range.

2. $S_T(q)$, the total scattering (in the absence of isotopic fluctuations), decreases rapidly with concentration. The ratio $S_T(q)/S_s(q)$ also decreases with increasing concentration, and that decrease is more rapid at low q . The very low values of that ratio at low q are a consequence of the apparent homogeneity of the solution on a scale of q^{-1} .

3. An interaction length, L_i , is defined as that value of q^{-1} at which $S_T(q) = |S_p(q)|$. In these experiments, L_i varies with $c^{-0.73}$. This variation is akin to that found for the screening length ξ , which varies as $c^{-0.70}$. See ref 1.

4. Agreement between the Benoit-Benmouna theory and these experiments is relatively good in the range 0.03

$< c < 0.16$. At high concentration, experimental error in $S_T(q)$ is too large to permit a serious test of the theory. At low concentration, discrepancies arise from experimental errors and, perhaps, because molecular overlap is insufficient for the theory to apply.

5. In the Benoit-Benmouna theory, the excluded volume parameter varies with c^n . The experiments yield $0.5 < n < 0.6$. Scaling theory yields a value of n between 0.25 and 0.41, depending on the parameter ν chosen for the relation $R \sim M^\nu$.

Acknowledgment. This work was supported by National Science Foundation Grant No. DMR-8217460.

References and Notes

- (1) King, J. S.; Boyer, W.; Wignall, G. D.; Ullman, R. *Macromolecules* **1985**, *18*, 709.
- (2) Zimm, B. H. *J. Chem. Phys.* **1948**, *16*, 1093.
- (3) Jannink, G.; de Gennes, P.-G. *J. Chem. Phys.* **1968**, *48*, 2260.
- (4) Benoit, H.; Benmouna, M. *Polymer* **1984**, *25*, 1059.
- (5) Akcasu, A. Z.; Summerfield, G. C.; Jahshan, S. N.; Han, C. C.; Kim, C. Y.; Yu, H. *J. Polym. Sci., Polym. Phys. Ed.* **1980**, *18*, 863.
- (6) Benoit, H.; Koberstein, J.; Leibler, L. *Makromol. Chem., Suppl.* **1981**, *4*, 85.
- (7) Koehler, W. C.; Hendricks, R. *J. Appl. Phys.* **1979**, *50*, 1951.
- (8) Child, H. R.; Spooner, S. J. *J. Appl. Crystallogr.* **1980**, *13*, 259.
- (9) des Cloizeaux, J. *J. Phys. (Les Ulis, Fr.)* **1975**, *36*, 281.
- (10) Einstein, A. *Ann. Phys. (Leipzig)* **1910**, *33*, 1275.
- (11) Debye, P. *J. Appl. Phys.* **1944**, *15*, 338.
- (12) Flory, P. J. *J. Chem. Phys.* **1949**, *17*, 303.
- (13) LeGillou, J. C.; Zinn-Justin, J. *Phys. Rev. Lett.* **1977**, *39*, 95.
- (14) Einaga, Y.; Miyake, Y.; Fujita, H. *J. Polym. Sci., Polym. Phys. Ed.* **1979**, *17*, 2103.

Effects of Polymer Structure and Incorporated Salt Species on Ionic Conductivity of Polymer Complexes Formed by Aliphatic Polyester and Alkali Metal Thiocyanate

Masayoshi Watanabe,* Masahiro Rikukawa, Kohei Sanui, and Naoya Ogata

Department of Chemistry, Sophia University, 7-1 Kioi-cho, Chiyoda-ku, Tokyo 102, Japan.
Received April 17, 1985

ABSTRACT: The effects of polymer structure and incorporated salt species on ionic conductivity were investigated in polymer complexes formed by aliphatic polyester and alkali metal thiocyanate (LiSCN, NaSCN, and KSCN). Poly(ethylene succinate) (PE-2,4) and poly(ethylene sebacate) (PE-2,10) were selected as the host polymers. The incorporated salts were dissolved in the amorphous region of the host polymers. The temperature dependence of the ionic conductivity did not show a single Arrhenius behavior but did show a Williams-Landel-Ferry type behavior. The ionic conductivity at a reduced temperature ($T_g + 90^\circ\text{C}$) was in the range of $(0.49\text{--}2.1) \times 10^{-6} \text{ S cm}^{-1}$ for the PE-2,4 complexes, depending on the incorporated salt species. The ionic conductivity at this reduced temperature for the PE-2,10 complexes was considerably lower than that observed in the PE-2,4 complexes and was $2.2 \times 10^{-8} \text{ S cm}^{-1}$ for the PE-2,10-LiSCN complex, $6.5 \times 10^{-10} \text{ S cm}^{-1}$ for the PE-2,10-NaSCN complex, and about $10^{-10} \text{ S cm}^{-1}$ for the PE-2,10-KSCN complex. The ionic mobility estimated from the transient ionic current method was $10^{-7}\text{--}10^{-6} \text{ cm}^2 \text{ V}^{-1} \text{ s}^{-1}$ at this temperature and was not affected greatly by the polymer structure and the incorporated salt species, which suggested that the free volume theory is valid for the ion transport in the polymer complexes. The lower ionic conductivity for the PE-2,10 complexes could be attributed to the lower number of carrier ions.

Introduction

Ion-conducting behavior in synthetic polymers has remained unclarified for a long time because ionic conductivity of usual polymers was extremely low and origin and kinds of carrier ions could not be exactly defined. However, relatively high ionic conductivity has recently been attained in certain kinds of ion-containing polymers.¹⁻¹⁰ Most of these ion-containing polymers are polymer complexes formed by host polymers and alkali

metal salts. The investigation of the ionic conductivity has gradually revealed the structure-conductivity relationships in these ion-containing polymers.

We have developed the method of ionic conductivity determination by means of complex impedance measurements,^{3,4,9} based on an appropriate equivalent circuit to interpret complex impedance diagrams, and have investigated structure-conductivity relationships in certain kinds of polymer complexes. Ionic conductivity, thus ob-